Swells of the East China Sea

Aifeng Tao[1,2], Jin Yan[2], Ye Pei[3], Jinhai Zheng[1,2] and Nobuhito Mori[4]

1. Key Laboratory of Coastal Disaster and Defence （Hohai University），Ministry of Education, Nanjing 210098, China

2. College of Harbor, Coastal and Offshore Engineering, Hohai University, Nanjing 210098, China

3. Xiangshui Yangtze Wind Power Generation Co.,Ltd, Xiangshui 224600, China

4. Disaster Prevention Research Institute, Kyoto University, Gokasho, Uji, Kyoto 611-0011, Japan

Corresponding author: Jinhai Zheng, email: jhzheng@hhu.edu.cn

Abstract

In the recent decades, more and more human activities, including different kinds of marine structures and large ships, have been present in the East China Sea. It is necessary to pay our attentions to the marine safety issues, particularly on the ocean waves. Because the waves have been known that the primary factor of marine safety and they may increase with Typhoon in the future with the global climate changing. The extreme waves can be induced not only by Typhoon in summer, but also by East Asian cold waves in winter for this special sea area. And the swells also can be very dangerous because swells may induce the resonance with floating structures, including the ships. Focusing on the investigation of swells in the East China Sea, the hindcast for waves in the past five years will be performed by the numerical model Wave Watch III based on the historical climate data. The numerical calculation domain covers the whole North West Pacific. Then the swells will be separated and analyzed from the simulated wave fields. Both the characteristics and the generation mechanisms of the swells will be investigated.

Keywords: Swell, East China Ocean, Propagation characteristic, Numerical simulation

1. Introduction

Swells are the waves remain on the sea when the sea wind stop or weaken or steering. And sometimes swells also come from the other waters. Compared to the wind waves, swell has a regular shape with large wave period, longer crest line and smooth wave surface. Because the amplitudes of heave and pitch are easy to be magnified by swells, the floating structures, such as the ships and floating platforms, are dangerous when they meet swells although the wave heights may lower compared with the wind waves. Sometimes it is called the resonance of floating structures induced by the swells. The changes of wave climate in the future have been investigated during the last decade (e.g., Hemer et al. 2014). And the results showed that there is a decreasing tendency for the wave heights over the Western North Pacific due to the global warming (Shimura et al., 2016). Shimura et al. (2013) showed the wave height climate responses to teleconnection patterns in the eastern part of the North Pacific and North Atlantic are more sensible than in the corresponding western parts. However, it is difficult to fine the results on the swells of the Western North Pacific, although the importance of swells has attracted more and more attentions.

In the East China Sea, the marine shipping is developed and there are many marine projects. These marine engineering are often affected by swell during the process of construction and operation. While the previous studies focus rarely on the swells. Therefore, it is necessary to investigate on the swells for the safety of marine navigation, the development and utilization of marine resources, the prevention and reduction of wave disasters.

The East China Sea is located in the East Asian monsoon region of the Northwest Pacific, which is affected by the monsoon all the year round. And in summer and winter, it will be subject to typhoons and cold waves and other extreme weathers. The effects of different meteorological conditions on the generation mechanism and evolution characteristics of the swells in East China Sea will be considered here. In addition, it had been observed that swell can spread from the

North Pacific to the northern part of Indian Ocean, through the latitude of 30 degrees (about 14422.2km) with little loss of energy (*Munk*, 1957). Thus the swells of the East China Sea could be induced by the local wind and may propagate from the east side of the Ryukyu chain. Then the influences of different calculation space scales will be considered in order to make clear the generation mechanisms of the swells in the East Chinas Sea. The numerical wave model of the East China Sea based on WaveWatch III will be established and validated. The results will be analyzed for both the characteristics and generation mechanisms of the swells.

2. Data and Methodology

2.1. Model Setup

The official version 3.14 of WAVEWATCH III (hereinafter WW3) is used here (*Tolman*, 2009). Water depths are derived from the NGDC (National Geophysical Data Center) ETOPO 1 data (*Amante et al*., 2009) and the resolution is 1/60 °×1/60 °. The wind field data are derived from CCMP/NCEP & Myers (*Liu et al.*, 2011; *Milliff et al.*, 2004; *Myers*, 1954) datasets which are regularly gridded with a 6-hour interval and a resolution as 0.25 °×0.25 °. The typhoon data is derived from CMABST datasets (*Ying et al*., 2014).

The model grid is regular in latitude and longitude with 0.25 °×0.25 ° resolution. Source terms for energy spectra in the model are set to default. The spectral grid uses 24 directions regularly spaced over a full circle with a directional resolution of 15 °, and 24 frequencies from 0.04118 Hz to 0.40561 Hz, exponentially spaced with a factor of 1.1 of increment. All the parameters including significant wave height (hereinafter SWH), spectrum peak period (hereinafter SPP), and mean wave direction and so on are extracted from dimensional spectrum for both wind waves and swells.

Based on WW3 model, two calculation domains are considered within the Northwest Pacific, as shown in Figure 1. One is named as D1(0 °-50 °N, 100 °-160 °E) and the other one is D2(24 °-41 °N, 117 °-131 °E). These two spatial scales are selected for the analysis of the resources of swells in the East China Sea. The time duration of the hindcast is from January 1st, 2010 to December 31st, 2014. All the scenarios, including both typhoon and monsoon climates, are realized in both D1 and D2 with same spatial resolution as 0.25 °×0.25 and time step of 3600 s. The statistical parameters are output each 10800 s.

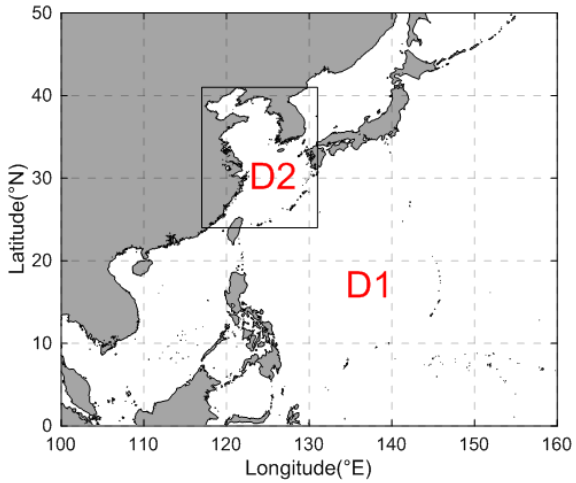

Figure 1. Numerical calculation domains. The larger domain is D1, and the smaller one is D2.

2.2. Model verification

As mentioned above, the source terms of the model are set to be default. So that it is necessary to verify the feasibility of numerical wave model before running the numerical realizations (*Hanson et al.*, 2009). It is more reasonable to verify the swells directly by the comparison between the numerical results and observed data. Unfortunately, it is difficult to get the observed data of swells since most of the data are only about the combined waves. The observed wave data used here for model verification are also ~~for~~ the combined wave data. And it should be trusted for the capture

abilities of the swells because the separation approach of wind waves and swells, which is used in the version 3.14 of WW3, has already been verified in details by Tracy (*Tracy et al.*, 2007).

The physical parameters of both the significant wave height and the spectrum peak period are used to verify the wave model established in the whole Northwest Pacific Ocean based on observed data from two stations. As figure 2 shown, The first station Xiangshui is outside of Xiangshui of Jiangsu Province, China. The second station Ikitsuki is outside of the Ikitsuki Island of Japan. The simulation durations and related climates are shown in Table 1.

Table 1. Information of two observation stations

station	Observed data duration	Location(Longitude, Latitude)	Mean water depth (m)	Related climate
Xiangshui	2011.01.01-2011.01.31	120°6′E, 34°26.2′N	8.4	Regular
Ikitsuki	2012.08.10-2012.10.09	129 °25.8′E, 33 °26.4′N	91	Typhoon & Regular

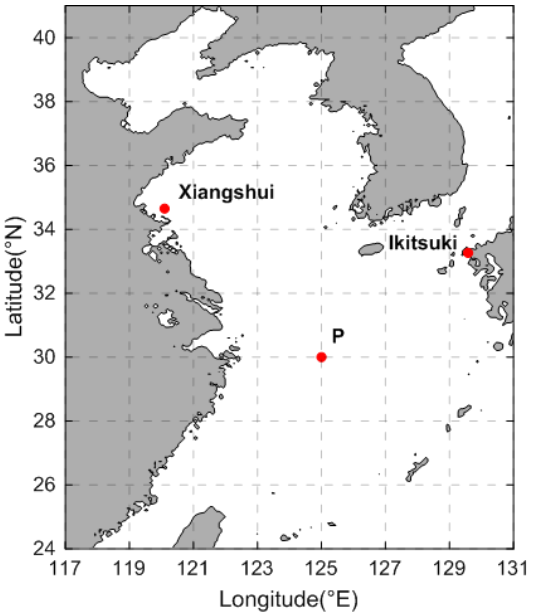

Figure 2. Locations of the observation stations and point P.

The comparison results between simulated values and measured data are shown in Figure 3. It is shown that the simulation results are fairly well agreed with observations throughout the two stations in terms of time-varying patterns. The correlation coefficient, the bias, the mean absolute error and the root mean square error between the simulated and measured values were calculated to quantify the comparison results, and shown in Table 2. The correlation coefficients (CC) are all larger than 0.8, which indicates the correlation between the simulated and measured values are satisfied. From the calculation results of the bias, the results of the two stations are positive and the values are relatively small, which indicates that the simulated value of WW3 is slightly larger than the measured value. On the mean absolute error (MAE) and root mean square error (RMSE), both values are also relatively small and in the allowable range of the specification. In summary, it is considered that the simulation results of the model are in good accordance with the observations, and the WW3 wave model can be used to simulate the wave fields in the East China Sea.

Table 2. Statistical results of the comparison between measured data and simulated values.

Buoy Stations		Statistical Parameters			
		CC	Bias	MAE	RMSE
Xiangshui	SWH	0.96	0.05	0.79	0.58
	SPP	0.92	0.38	0.87	0.63
Ikitsuki	SWH	0.85	0.02	0.45	0.49
	SPP	0.82	0.06	0.57	0.61

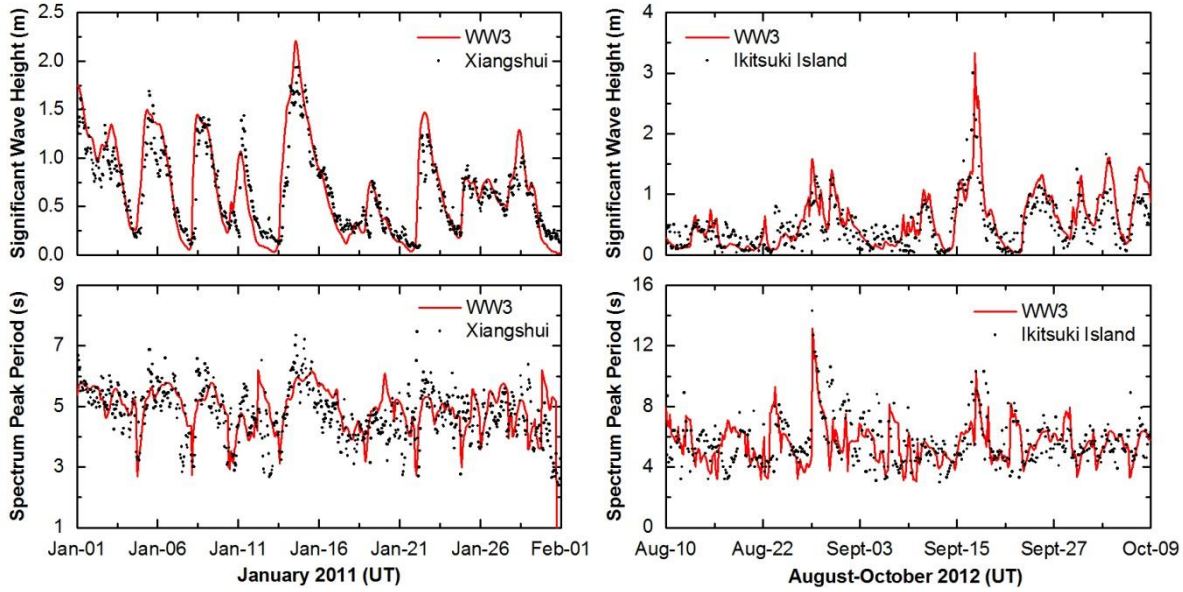

Figure 3. **Comparison between the measured data and simulated values.** Observation and simulation are identified with scatter and line respectively over time

2.3. Swell Separation

A wave age criterion was used to identify wind seas with the peak wind seas lie within the parabolic boundaries defined by (*Hanson et al., 2000*):

$$C_p \leq (1.5)U_{10}\cos\delta \tag{1}$$

where C_p is the phase speed of the wind sea, U_{10} is the 10-m elevation wind speed, and δ is the angle between the wind and the wind sea. In terms of the peak frequency of the wind sea peak in deep water, the equation above becomes:

$$f_p \geq \frac{g}{2\pi}[1.5U_{10}\cos\delta]^{-1} \qquad 0 \leq \delta \leq 2\pi \tag{2}$$

The generous factor of 1.5 ensures that all possible wind sea peaks are included.

3. Result analysis

3.1. Spatial and Temporal Distribution of Swell in East China Sea

3.1.1. Temporal Distribution of the Swell in East China Sea

For the convenience of comprehending the maximum likelihood significant wave heights and correlative spatial distribution of swell, here we use sea state (WMO Sea State) to depict the swells in East China Sea. A typical representative point labeled as P (125 ° E, 30 ° N), which ~~point~~ is shown in Figure 2, was selected to analyze the evolution of swell on a time scale. The time range of the simulation data chosen to be analyzed is the whole year of 2011, as the example.

To illustrate the effects of the extreme climate on the swells, the wave evolution processes during the typhoon 'Muifa' are shown in Figure 4. It can be seen that when the typhoon moved close to D2 from July 29th to August 4th, the swell was in domination at P-point, and its significant wave height is about 1 m, and the spectrum peak periods of swells were mainly distributed in 9-14 s. With the typhoon gradually approaching P-point, its effect on the East China Sea also increased. From August 4th to August 8th, the waves of P-point were transformed into wind sea without swell. After typhoon moving away from P-point, swell continued to become a part of mixed wave.

The swells at P-point are computed for monthly, quarterly and annual averages to illustrate temporal distribution characteristics. The monthly averaged significant wave heights of swells are mainly less than 1.2 m with higher values in February, July and August. The monthly average spectrum peak periods of swells are mainly seldom reach 12 s, which are larger in February, September and December. The swells in the third quarter are the highest, and the quarterly

average significant wave heights of swells are mainly less than 1.0 m, and the quarterly average spectrum peak periods of swells are mainly less than 10 s. The annual averaged values from 2010 to 2014 are also investigated in order to catch the inter-annual variability of the swell in the East China Sea. The annual averaged significant wave heights are mainly distributed in 0-1.0 m, and the annual average spectrum peak periods of swells are mainly distributed in 0-10 s. By comparison, the temporal distribution of swell in different years is similar, and the differences are small.

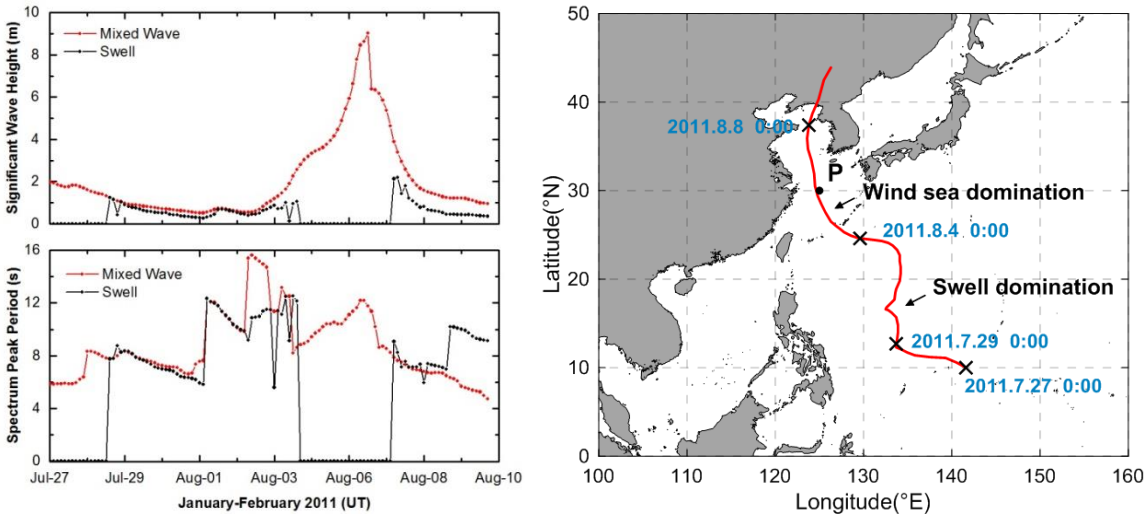

Figure 4. The comparison between mixed wave and swell at P-point and movement path of typhoon 'Muifa'. Mixed wave and swell at P-point are identified with different color.

To understand the distribution of swell under different weather conditions quantitatively, the statistics and analysis of the frequency of swell are given below. During non-typhoon scenarios, the significant wave heights of swells in the East China Sea are mainly distributed in the interval of 0.1-1.25 m (in figure 5), the interval with the highest frequency of occurrence is 0.1-0.5 m, and the proportion of is 54.0%.The same as non-typhoon scenarios, the significant wave heights are mainly distributed in the 0.1-4.0 m during typhoon seasons, however, the interval with the highest frequency of occurrence is 0.5-1.25 m, which occupies 49.5% of time in a year.

Spectrum peak periods, as shown in Figure 5, are mainly distributed in the section of 4-15 s during non-typhoon scenarios. The interval with the highest frequency of occurrence is 8-15 s, with a proportion as about 22%. In addition, during typhoon scenarios, the spectrum peak periods are mainly distributed in the interval of 4-30 s. The interval with the highest frequency of occurrence is 8-15 s, and the proportion is 27.9%.

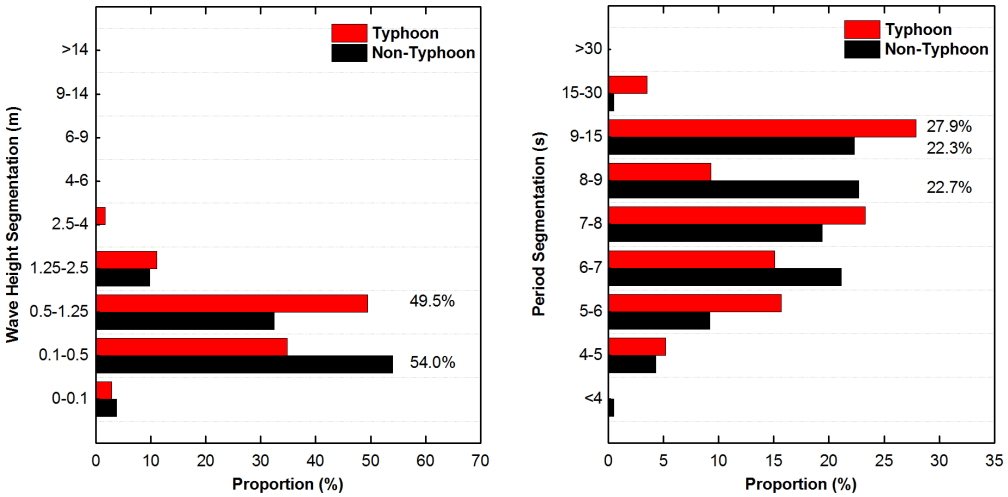

Figure 5. The proportion of each sea state in typhoon and non-typhoon scenarios during 2010. (a) is significant wave height, (b) is spectrum peak period.

The proportion of each state from 2010-2014 was computed to reveal the annually variation of swells, as shown in Figure 6. Obviously, the main properties of the distribution ranges are consistent although the corresponding frequencies are not exactly the same. The significant wave heights of swells in the East China Sea are mainly distributed in the 0.1-2.5 m, with a highest frequency interval as 0.1-0.5m and the proportion is about 49%.The distribution range of spectrum peak periods is 4-15 s, and the maximum possible interval is 9-15 s.

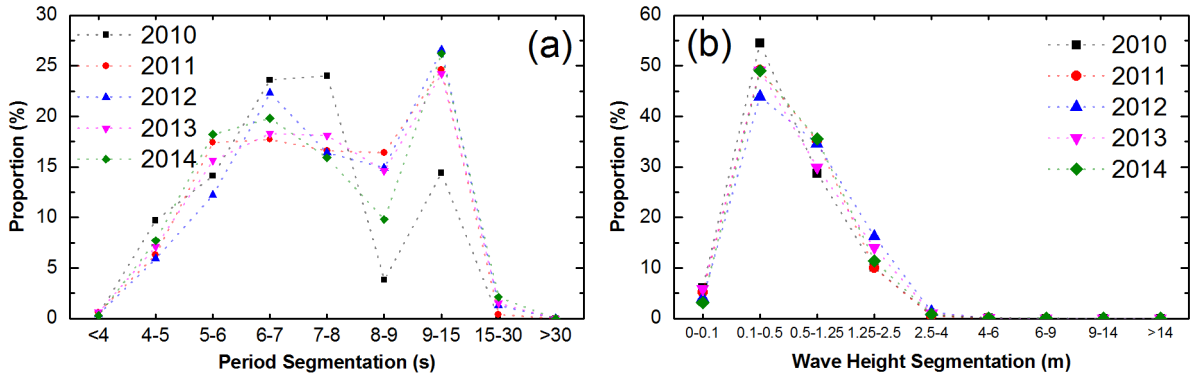

Figure 6. The proportion of each sea state during 2010-2014. (a) is spectrum peak period, (b) is significant wave height.

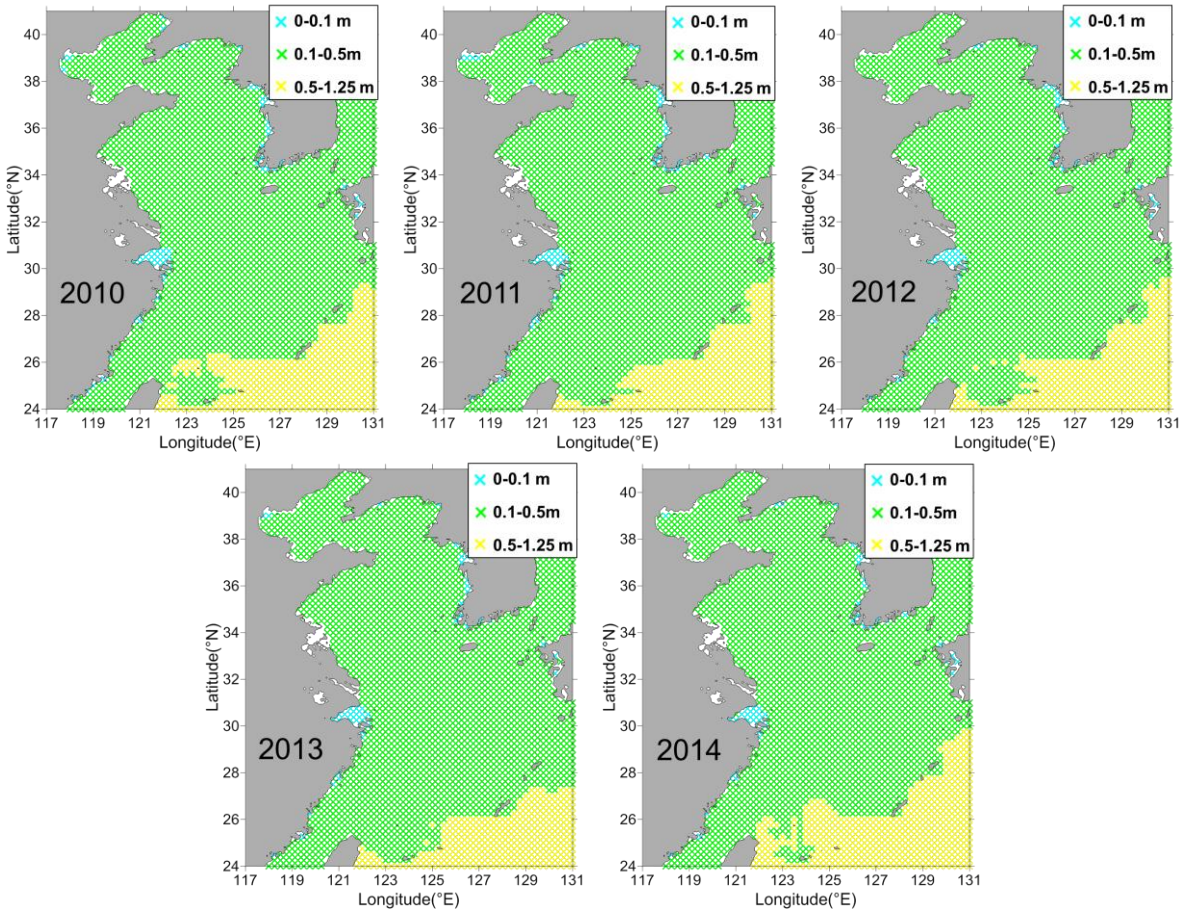

Figure 7. Spatial distribution of the maximum likelihood significant wave heights of swells in 2010-2014

3.1.2. Spatial Distribution of the Swell in East China Sea.

The swell data of 2011 was used to illustrate the spatial distribution as an example. Sea state produced by swell of few offshore sea areas are code 1 (0-0.1 m) (in figure 7). Most sea areas present a same sea state as code 2 (0.1-0.5 m), and the sea states of areas outside Okinawa Trough are almost code 3 (0.5-1.25 m). The swells within the East China Sea

varied in the range of 0.1-0.5 m, which suggests that the energy of the swells in the East China Sea is relatively lower. In addition, the swells in the sea outside the Ryukyu chain are significantly higher, which indicates there is a blocking effect of the chain. It also can be seen from Figure 7 that the spatial distribution characteristics of the significant wave heights of swells for the simulated five year are all most constant. It can be assumed that, as least in the statistical viewpoint, the spatial distribution characteristics of the significant wave heights of swells are mainly owing to the effect of topography. It will be investigated in details in another paper.

The maximum likelihood spectrum peak periods of the swell in 2011 were also investigated as shown in Figure 8. Most areas outside the Ryukyu chain and half part of the East China Sea are labeled as code 7 (9-15 s). When the swells closing to the islands belong to the Ryukyu chain, the spectrum peak periods present a decreasing trend, especially in the northwest side of the chain. Compared to the areas outside the chain, half part of areas inside the chain are labeled under code 7, which means the swells belong to these areas are in high possibility varying in a range of 0-9 s. The period distribution illustrates a trend that spectrum peak period increasing from the offshore to the deep sea and from the North to the South.

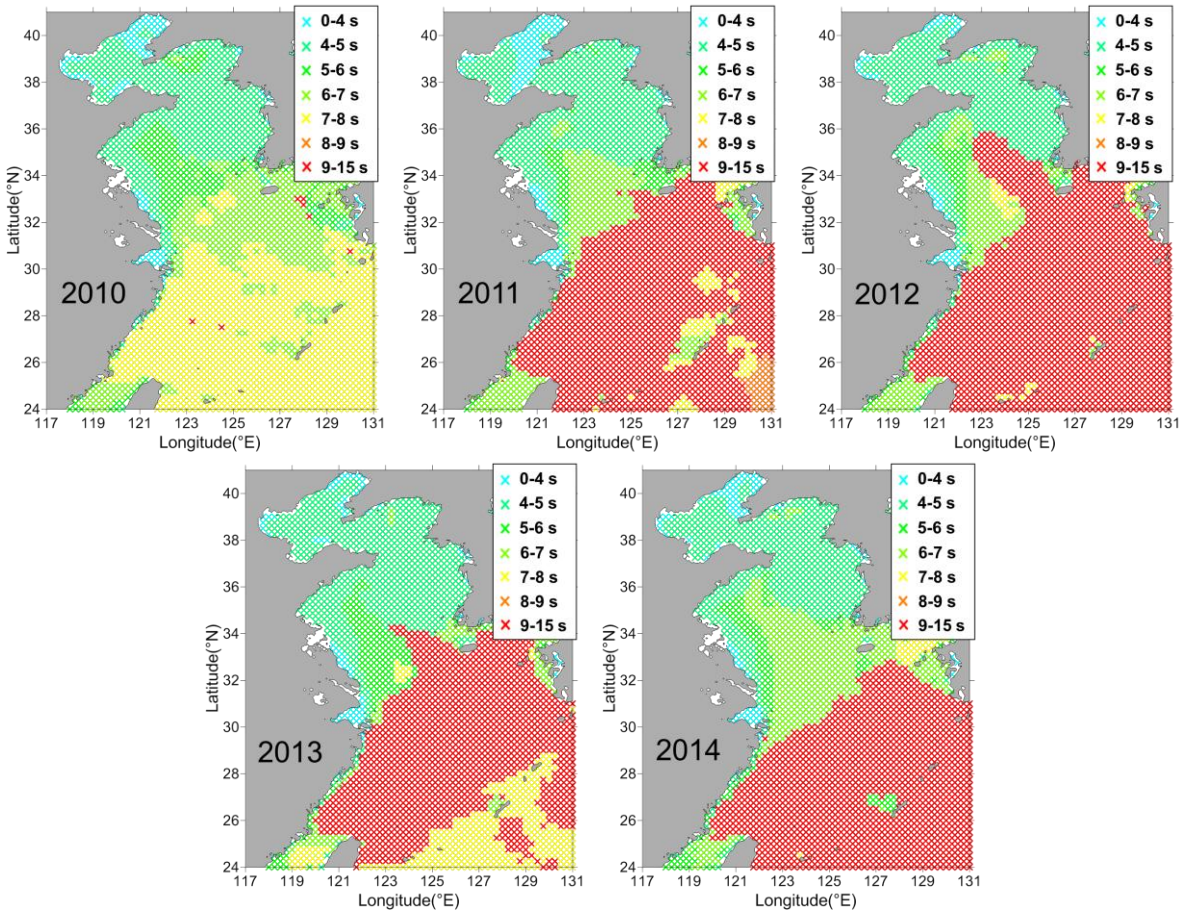

Figure 8. Spatial distribution of the maximum likelihood spectrum peak period of swells in 2011.

Unlike significant wave height distribution of swells, some differences for spectrum peak period distribution are present. It can be seen that swells with code 5 (7-8 s) were dominated in most part of the East China Sea in 2010, while the swells with code 7 (9-15 s) were dominated in 2011 to 2014. And the swells dominated outside the Ryukyu chain in 2010 and 2013 were code 5, which in 2011, 2012 and 2014 were code 7.

3.1.3 The relationship between typhoon and swell

During the simulated 5 years, there were totally 114 recorded typhoons in Northwest Pacific Ocean, but the effect days of typhoon were different, which is considered here. The details are shown in Figure 9. The annual mean significant wave height of swell ~~significant wave height~~ at P-point was computed to make a comparison between effect days of typhoon and significant wave height of swells. From Figure 9, it can be seen that the value of significant wave height of

swells increases with the number of extreme weather events. It can be proved that the length of typhoon effect is positive correlated with significant wave height of swells. While it is not a simply linear relation between those two parameters mentioned above. It should consider many factors such as typhoon moving path and so on.

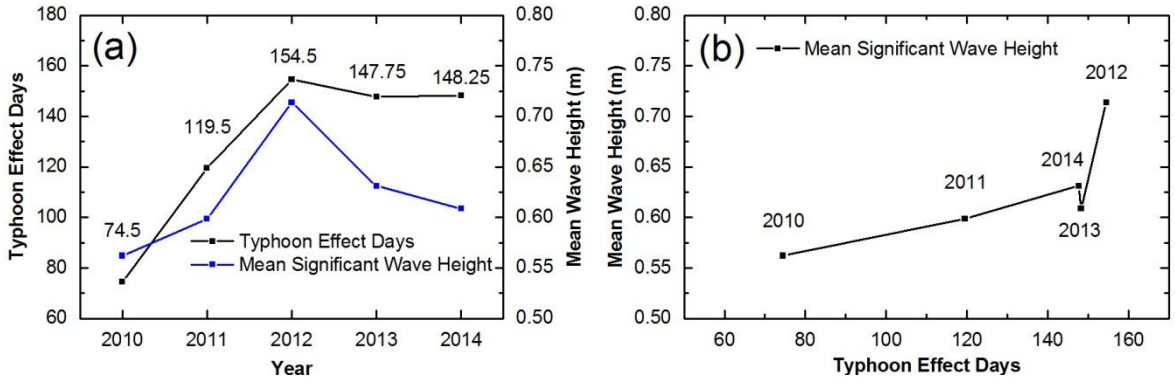

Figure 9. Relationship between typhoon and wave height. (a) is typhoon information among 2010-2014, (b) is the comparison between typhoon effect days and mean wave height of swell at P-point.

3.2. Generation mechanisms of the swells in East China Sea

The generation mechanisms of the swells were analyzed for typhoon and non-typhoon scenarios separately. Firstly, the simulation results with scale of D1 (Northwest Pacific) and D2 (East China Sea) are compared. From figure 10, it can be seen that the comparisons between results from different scales are mainly in four states. The first one is that the results are almost same for different scales. It means the swells are generated purely by the local wind of the small calculation sale D2, which is labeled as 'generated by local wind' hereinafter. The second one is that values of large scale are larger than those of small scale, while the values of small scale are not zero, which means part of the swells is propagated from outside of D2. This state is labeled as 'from both areas' hereinafter. The third one is that the values of large scale are non-zero values with zero values of small scale. It suggests all the swells are propagated from outside of D2. This state is labeled as 'from adjacent sea' hereinafter. The last one, labeled as 'no swells', is that the values of both scales are zero. It indicates there are no swells here at least in the consideration of large scale of D1.

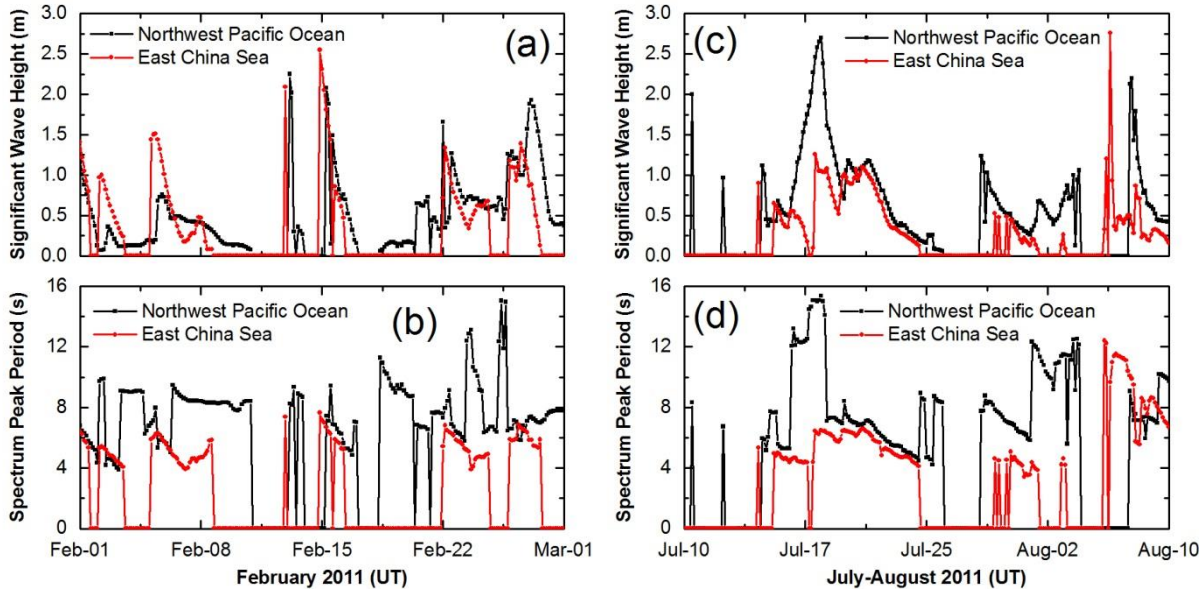

Figure 10. Calculated parameters of the swells from different spatial scales for non-typhoon and typhoon scenarios. (a) and (b) are for non-typhoon scenarios, (c) and (d) are for typhoon scenarios

The proportions of each swell state and corresponding ranges at P-point are calculated for the whole 2011 and the results are listed in Table 3 and Table 4 for non-typhoon and typhoon scenarios respectively. It can be seen that, during

non-typhoon scenarios, the swells generated by the local wind account for the largest proportion (38%). However, the swells come from the adjacent sea occupies the largest proportion (43%) during the typhoon scenarios. Both two kinds of scenarios present a common state that the significant wave heights and spectrum peak periods of swells generated by local wind is lower than that from adjacent sea and from both areas.

Table 3. Statistics for four swell states during non-typhoon scenarios of 2011 at P-point

swell states	proportion	variation range of characteristic parameters	
		SWH(m)	SPP(s)
come from adjacent sea	21%	0.06~2.55	4.5~15.0
generated by local wind	38%	0.07~1.53	4.0~10.0
from both areas	29%	0.08~2.08	5.0~13.0
no swells	12%	/	/

Table 4. Statistics for four swell states during typhoon scenarios of 2011 at P-point

swell states	proportion	Variation range of characteristic parameters	
		SWH(m)	SPP(s)
come from adjacent sea	28%	0.06~2.03	5.0~15.0
generated by local wind	13%	0.21~1.15	4.5~8.0
from both areas	43%	0.26~2.70	5.0~15.5
no swells	16%	/	/

In order to understand the variations among different years, a statistic analysis of the simulation results throughout the East China Sea during 2010-2014 is made in this paper. The composition of swell at P-point in 2010-2014 is presented in Table 5. It can be seen that in a half of a year, the swells at P-point are composed of both swells generated by the local wind field and swells come from the adjacent sea. In about 25%-30% of a year, the swells at P-point only propagate from the adjacent sea. The swells at P-point are only generated by the local wind field for a small percentage of time in a year. And in the rest of a year there is no swell at P-point. In addition, the differences of the compositions of swell among different years are small.

Table 5. Composition of swell in East China Sea in 2010-2014.

Composition of Swell	Proportion					
	2010	2011	2012	2013	2014	average
Come from adjacent sea	34%	36%	25%	23%	22%	28%
Generated by local wind	5%	3%	4%	4%	5%	4%
Both common composition	39%	37%	49%	49%	55%	46%
No swell	22%	24%	22%	24%	18%	22%

4. Conclusions and discussion

Based on the Wave Watch III numerical model and the basic data from Etop1, CCMP, the wave fields of North West Pacific, particularly the East China Sea, were simulated from 2010 to 2014. After separating swell and wind sea from mixed waves, the spatial and temporal distribution of swell and the mechanism of swells in East China Sea were investigated. The significant wave heights of swells in the East China Sea are mainly distributed in the 0.1-2.5 m, the interval with the highest frequency of occurrence is 0.1-0.5 m, and the proportion is about 50%. The spectrum peak periods of swells are mainly distributed in the 4-15 s, the interval with the highest frequency of occurrence is 9-15 s., and the proportion is about 25%. In terms of spatial distribution，swells increase gradually from the offshore to deep sea, and also increase gradually from the north to the South. Moreover, the values of swells in the sea outside the Ryukyu Chain are significantly greater than the values of swell in the area within Ryukyu Chain. The spatial distributions of swells among different years present a high similarity.

The swells in East China Sea are affected by the local wind in East China Sea and swells come from other adjacent sea

areas. From the composition analysis of influence factors under different meteorological conditions, it can be seen that during the non-typhoon scenarios, the swells generated by the local wind account for the largest proportion, accounting for about 38% of the simulation time zone. During the typhoon scenarios, the swells come from the adjacent sea account for the largest proportion, which is about 43% of the simulation time zone. From the composition analysis of influence factors of a year, it is known that in about a half of a year, the swells in East China Sea are composed of swells generated by the local wind field and swells come from the adjacent sea. In about 25%-30% of a year, the swells in East China Sea are only propagating from the adjacent sea. However, the swells in East China Sea are only generated by the local wind field for a small percentage of time in a year. It needs to be emphasized that the existence of swells are common phenomena, since the swells are present more than third quarters of a year. Thus the research works related swells of East China Sea are meaningful.

Acknowledgments

This research work is funded by the National Natural Science Fund (51579091, 51379071, 51137002), the National Science Fund for Distinguished Young Scholars (51425901)，the Qing Lan Project of Jiangsu Province, the Basic Research Fund from State Key Laboratory of Hydrology-Water Resources and Hydraulic Engineering, Hohai University (20145027512 and 20145028412), the Short-term Research Visits project supported by Disaster Prevention Research Institute of Kyoto University (27S-02), the Fundamental Research Funds for the Central Universities of Hohai University (2016B05214).

Reference

AMANTE C, EAKINS B W. ETOPO1 1 Arc-Minute Global Relief Model: procedures, data sources and analysis[J]. *Psychologist*, 2009, 16(3): 20 -25.

Bartsch H J, Hays D F. Handbook of mathematical formulas[J]. *Handbook of Mathematical Formulas*, 1974(2):3.

Hanson J L, Phillips O M. Automated Analysis of Ocean Surface Directional Wave Spectra[J]. *J.atmos.oceanic Technol*, 2001, 18(2):277-293.

Hanson J L, Tracy B A, Tolman H L, et al. Pacific Hindcast Performance of Three Numerical Wave Models[J]. *Journal of Atmospheric & Oceanic Technology*, 2009, 26(26): 1614-1633.

Hemer, M.A., Y. Fan, N. Mori, A. Semedo and X.L.Wang (2013) Projected changes in wave climate from a multi-model ensemble, Nature Climate Change, 6p., doi:10.1038/nclimate1791.

Liu Z H, Zheng C W, Zhuang H, et al. Long-Term Trend and Special Characteristics of Sea Surface Wind Speed in the Northwest Pacific Ocean During the Last 22 Years[J]. *Ocean Technology*, 2011, 02: 127-130.

Milliff R F, Morzel J, Chelton D B, et al. Wind Stress Curl and Wind Stress Divergence Biases from Rain Effects on QSCAT Surface Wind Retrievals[J]. *Journal of Atmospheric & Oceanic Technology*, 2004, 21(8): 1216-1231.

Munk W H, Snodgrass F E. Measurements of southern swell at Guadalupe Island[J]. *Deep Sea Research*, 1957, 4(4): 272-286.

Myers V A. Characteristics of United States hurricanes pertinent to levee design for Lake Okechobeem[R]. *F L Hydro met Report 32*. Government Printing Office, 1954.

Shimura T., N. Mori and H. Mase (2013) Ocean waves and teleconnection patterns in the Northern Hemisphere, Journal of Climate, American Meteorological Society, 26, pp.8654-8670.

Shimura T., N. Mori and M.A. Hemer (2016) Variability and future decreases in winter wave heights in the Western North Pacific, Geophysical Research Letters, 10.1002/2016GL067924.

Tolman H L. User manual and system documentation of WAVEWATCH III version 3.14[J]. *Technical Note*, 2009, 166.

Tracy B, Devaliere E, Hanson J, Nicolini T, Tolman H. Wind sea and swell delineation for numerical wave modeling. Oahu: the 10th International Workshop on Hindcasting and Forecasting, 2007.

Ying M, Zhang W, Yu H, et al. An Overview of the China Meteorological Administration Tropical Cyclone Database[J]. *Journal of Atmospheric & Oceanic Technology*, 2014, 31(2):287-301.